JOURNAL OF GUIDANCE, CONTROL, AND DYNAMICS
Vol. 20, No. 2, March–April 1997

Strategy for the Passive Maneuvering of Tether-Connected Systems

Shi-Sheng Chu and Li-Sheng Wang
National Taiwan University, Taipei, Taiwan, Republic of China

New strategies for the deployment and the retrieval phases for tether-connected systems, such as the tethered satellite system, are presented. The passive strategy, which is similar in spirit to that of the idea of Hohmann transfer, takes advantage of the gravitational field. For the deployment, appropriate circular, elliptic, or hyperbolic orbits are designed for the spacecraft and the payload, respectively. The tether keeps slack during the process until being pulled taut at the final stage. Analogous strategies can be designed for the retrieval phase. Conditions on the designed transfer orbits are derived from the orbital equations and Kepler's equation. Numerical results show that such methodologies have potential applications.

I. Introduction

SINCE the idea of using a long tether to deploy a satellite from a spacecraft (e.g., the Space Shuttle) was proposed by Colombo et al.[1] in 1974, the dynamic behavior of the tethered satellite system (TSS) and the control strategies for a successful TSS mission have gained substantial considerations.[2–14] A typical TSS mission, e.g., the joint project of NASA and the Italian Space Agency flown on July 31, 1992, needs to deploy the payload from the spacecraft to a specific designed orbit. Then, with the spacecraft and the payload being at each end of the connecting tether, the assembly moves around the Earth in a stationary Earth-pointing attitude, at which the tether is along the radial direction. During this phase, the designed scientific experiments or measurements can be performed. Finally, for gathering the data or other purposes, the payload may be required to be retrieved back to the spacecraft via the tether. Therefore, the TSS maneuvers can be divided mainly into three phases: deployment, station keeping, and retrieval.

Consideration of the flexibility of the tether yields nonlinear and complex dynamical equations for the TSS, which can be very difficult to deal with. Thus, it is normally assumed in the analysis of control strategies that the tether remains in tension, i.e., the tension force along the tether is nonzero, so that it can be modeled as a length-varying rigid rod[12,15] or a series of rigid rods.[11,16] Based on this assumption and the linearized dynamical equations, various control algorithms for the aforementioned three phases[2,3] have been developed. Tether length control or tether tension control strategies for in-plane motions are proposed with observable states including tether length, length rate, in-plane (pitch) angle, angle rate, etc. The decoupled or partially decoupled out-of-plane motions are damped by suitable actuators, such as the thrusters,[17–19] which are also used to keep the tether taut. Such strategies are termed active control procedure in Ref. 3. On the other hand, Kane and Levinson[9] proposed a passive scheme for the deployment during which the payload moves freely in space after initial ejection until the tether becomes taut. However, some damping mechanism is needed at the final stage to keep the spacecraft and the payload in the Earth-pointing attitude.

New passive strategies of maneuvering for the deployment and the retrieval phases are proposed and analyzed in this paper. The idea, which is similar in spirit to that of the idea of Hohmann transfer, is to take advantage of the gravitational field. For the deployment, after the initial separation, suitable natural orbits, such as circular, elliptic, or hyperbolic orbits, are designed for the spacecraft and the payload, respectively. The tether keeps slack during the process until being pulled taut at the final stage. Based on the proposed strategy, various conditions on the transfer orbits for either the spacecraft or the payload are derived from the orbital equations

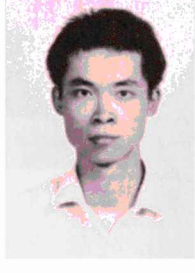

Shi-Sheng Chu received his B.S. degree in aeronautical and astronautical engineering in 1990 from National Cheng-Kung University and his M.S. degree in applied mechanics from National Taiwan University in 1992. He is currently pursuing his Ph.D. degree in applied mechanics from National Taiwan University. His current research interests include rolling contact problem, geometrical mechanics, sport mechanics, and aerospace applications.

Li-Sheng Wang received his B.S. degree from National Taiwan University in 1983 and his M.S. and Ph.D. degrees from the University of Maryland, College Park, in 1987 and 1990, respectively, all in electrical engineering. From 1990 to 1991, he held a research and teaching position at the Department of Mathematics, University of Maryland, College Park. Since 1991, he has been with the Institute of Applied Mechanics, National Taiwan University, where he is currently an Associate Professor. His research interests include nonlinear systems theory, geometrical mechanics, robotics, and aerospace applications. He is a Member of the AIAA.

Received Jan. 31, 1996; revision received Oct. 25, 1996; accepted for publication Oct. 28, 1996.

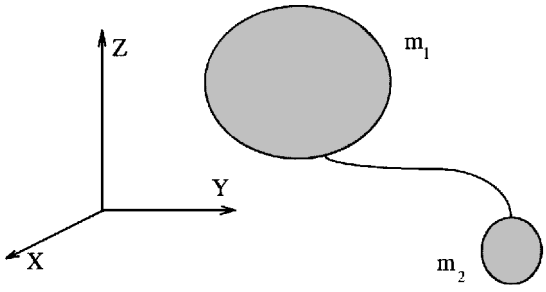

Fig. 1 System configuration.

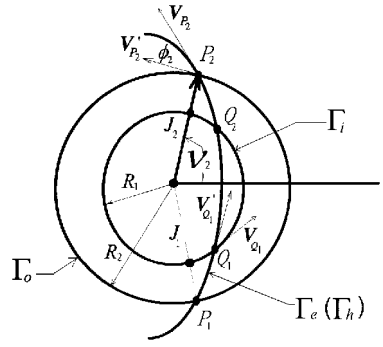

Fig. 2 Transfer orbit.

and Kepler's equation. Parameters of the desired orbits can then be obtained by performing numerical computations. Reverse procedures for deployment can be applied to the retrieval phase. Such methodologies not only save energy but also possibly enhance the reliability of the mission. Furthermore, it is shown that the mission can be achieved within one orbit of the spacecraft, which is faster than most other procedures.[2,11,19]

The contents are divided into the following sections. The system description appears in Sec. II. The system requirements for a successful strategy for the deployment phase are then discussed in Sec. III. The possibility of using elliptic orbits and hyperbolic orbits as transfer orbits are examined in Secs. III.A and III.B, respectively. A practical example for TSS deployment is discussed in Sec. IV, in which the orbital parameters, the ejection point, and the point of pulling are obtained. Section V discusses the retrieval phase, which is simply the reverse process of the deployment phase. Some concluding remarks are given in Sec. VI.

II. System Description

The problem at hand is to study the possibility of using some transfer orbits to bring the payload from the spacecraft to a required orbit, or vice versa, for a tether-connected system. The system is modeled as two particles, m_1 and m_2, connected by a long tether (the length of the tether could be extended to 100 km or more), where m_1 and m_2 denote the masses of the spacecraft and the payload, respectively, with the assumption of $m_1 \gg m_2$ (Fig. 1).

Prior to the deployment of the payload, this assembly is assumed to move around the Earth in a fixed circular orbit with the tether wound on a reel mechanism inside the spacecraft. The objective of the deployment is to put the payload at a designated circular orbit, with the final configuration of the assembly in the Earth-pointing radial position, which is proved to be a stable steady motion under certain conditions.[20] However, some disturbances may possibly cause the TSS system to deviate from the Earth-pointing configuration. The station-keeping phase is then not only to keep the spacecraft and the payload in their desired orbits but also to maintain the stable radial configuration. The other operational phase for TSS is to retrieve the payload from the outer orbit to the spacecraft, which is termed the retrieval phase.

It is assumed that the spacecraft is equipped with thrusters and the motion of the system is subjected to the central gravitational force.

III. Deployment Strategy

According to the system description in Sec. II, it is necessary to set up a deployment strategy to construct a bridge between the initial and the final configuration. From the idea of the Hohmann transfer orbit, a scheme is proposed, as shown in Fig. 2, where the inner circular orbit (with radius R_1, denoted by Γ_i) is the one before deployment, while the outer one (with radius R_2, denoted by Γ_o) is the destination for the payload.

The goal is to find suitable transfer orbits so that the following strategy for the deployment may be taken.

1) Give an impulse to the payload in a specific direction at the point Q_1 or Q_2, such that it can move along the transfer orbit to the point P_2.

2) After the ejection of the payload, the spacecraft must reach the position J_2 such that the tether is in radial configuration when the payload arrives at P_2.

3) When the spacecraft arrives at J_2, impose a suitable impulse on the payload via the tether such that the velocity of the payload at P_2 can be changed to the velocity of Γ_o at P_2, i.e., $\boldsymbol{V}'_{P_2}$.

It can be easily verified that a circle and an ellipse (or a hyperbola) with the same focus can intersect at no more than two points, which are $\{Q_1, Q_2\}$ and $\{P_1, P_2\}$ for Γ_i and Γ_o, respectively. The two points may degenerate to one point when the transfer orbit is tangent to the circular orbit at the perigee or apogee, which is the case for Hohmann transfer.

Here, we deal only with the problem of sending the payload outward from the spacecraft. Two possibilities for the transfer orbit, namely, elliptic orbits and hyperbolic orbits, are discussed in Secs. III.A and III.B, respectively. It is shown that an orbital change of the spacecraft as well as the payload during the process may be needed.

A. Elliptic Orbits

1. Ejecting the Payload at Q_1

First, we consider the case that the payload is ejected at Q_1 via an elliptic orbit Γ_e, while the spacecraft is kept in the inner-circular orbit Γ_i. Let a be the semimajor axis, e be the eccentricity, and H denote the magnitude of angular momentum per unit mass of Γ_e. We have

$$H = \sqrt{a\mu(1-e^2)}$$

where μ is the gravitational constant. The radius of the elliptic orbit is

$$r = \frac{H^2/\mu}{1 + e\cos\nu}$$

where ν denotes the true anomaly. The intersection of Γ_o and Γ_e at P_2 requires

$$R_2 = \frac{H^2/\mu}{1 + e\cos\nu_2} \tag{1}$$

where ν_2 denotes the true anomaly of P_2 with respect to Γ_e. The conservation of angular momentum along Γ_e implies

$$\sqrt{a\mu(1-e^2)} = R_2\sqrt{\mu[(2/R_2) - (1/a)]}\cos\phi_2 \tag{2}$$

where ϕ_2 is the angle between the velocity of Γ_e and that of Γ_o at P_2. Furthermore, to be able to change the velocity of the payload from $\boldsymbol{V}_{P_2}$ to $\boldsymbol{V}'_{P_2}$ by pulling the tether along the radial direction, we impose the condition

$$\sqrt{\mu/R_2} = \sqrt{\mu[(2/R_2) - (1/a)]}\cos\phi_2 \tag{3}$$

where the left-hand side (LHS) is the magnitude of the velocity $\boldsymbol{V}'_{P_2}$. On the other hand, it is required that when the payload reaches P_2, the spacecraft must move to J_2 so that the vector from $\boldsymbol{J}_2$ to $\boldsymbol{P}_2$ is along the radial direction. First, we compute the time elapsed for the payload moving from Q_1 to P_2 along Γ_e. Let $-E_1$ and $-M_1$ denote the eccentric anomaly and the mean anomaly of Q_1, respectively, with E_1 and $M_1 \geq 0$, and let E_2 and M_2 denote the

eccentric anomaly and the mean anomaly of P_2, respectively. We have

$$-M_1 = -E_1 + e\sin E_1 = \sqrt{(\mu/a^3)}(t_1 - T_0)$$

$$M_2 = E_2 - e\sin E_2 = \sqrt{(\mu/a^3)}(t_2 - T_0)$$

where T_0 denotes the perigee time.[21] Accordingly, the time required for the payload to reach P_2 is $t_2 - t_1$, i.e.,

$$\sqrt{(a^3/\mu)}[(E_2 - e\sin E_2) + (E_1 - e\sin E_1)]$$

Second, the time for the spacecraft moving from Q_1 to J_2 along Γ_i is

$$\sqrt{\left(R_1^3/\mu\right)}(\nu_2 - \nu_1)$$

where ν_1 is the true anomaly of Q_1 with $\nu_1 \le 0$. As a result, we have the equal-time condition

$$\sqrt{(a^3/\mu)}[E_1 + E_2 - e(\sin E_1 + \sin E_2)] = \sqrt{\left(R_1^3/\mu\right)}(\nu_2 - \nu_1) \tag{4}$$

It is necessary to find a, e, ν_1, and ν_2 such that all four conditions (1–4) are satisfied. From Eqs. (1–3), it can be shown that

$$R_2 = a(1 - e^2) \qquad \text{and} \qquad \cos\nu_2 = 0$$

which implies $\nu_2 = \pi/2, 3\pi/2, 5\pi/2$, etc., i.e., R_2 is the semilatus rectum of the transfer orbit. Recall that for the Hohmann transfer orbits, the true anomaly of P_2 is π; thus, the discussion here excludes the possibility of using Hohmann transfer orbit in our strategy. By the identity

$$\cos E = \frac{e + \cos\nu}{1 + e\cos\nu}$$

we have

$$E_2 = \arccos e \pm 2\pi$$

Because of the tether length constraint, we choose $\nu_2 = \pi/2$, $E_2 = \arccos e$. Condition (4) can be expressed as

$$\sqrt{(a^3/\mu)}\left[(E_1 + \arccos e) - e\left(\sqrt{1 - e^2} + \sin E_1\right)\right] = \sqrt{\left(R_1^3/\mu\right)}[(\pi/2) - \nu_1] \tag{5}$$

From the identities

$$R_1 = \frac{a(1 - e^2)}{1 + e\cos\nu_1}, \qquad \cos E_1 = \frac{e + \cos\nu_1}{1 + e\cos\nu_1}$$

and defining

$$K = \frac{R_2 - R_1}{R_1} \tag{6}$$

Eq. (5) can be rewritten as

$$\left(\arccos e - e\sqrt{1 - e^2}\right) - \left(\frac{1 - e^2}{1 + K}\right)^{1.5}\left(\frac{\pi}{2} + \arccos\frac{K}{e}\right) = -\arccos\left[\frac{[e + (K/e)]}{1 + K}\right] + \frac{\sqrt{1 - e^2}\sqrt{e^2 - K^2}}{1 + K} \tag{7}$$

with $(K/e) \le 1$. Thus, the eccentricity of the elliptic orbit must be greater than $(R_2 - R_1)/R_1$. Given R_1 and R_2, we can then compute e by using Eq. (7). For some selected R_1 and R_2, the numerical results are shown in Table 1. It is noted that as K approaches zero, the eccentricity goes to zero, i.e., the transfer orbit approaches a circle. Moreover, the transfer orbits for the cases with the same value of K have the same eccentricity, regardless of different pairs of R_1 and R_2.

Table 1 Possible transfer orbit Γ_e

R_1, km	R_2, km	K	e
6800	6900	0.1470	0.1575
6800	6880	0.1176	0.1259
6800	6850	0.07352	0.07872
6800	6820	0.02941	0.03147
6800	6800.25	0.0003676	0.0003934

With the algorithm just proposed, it is interesting to know the required change of the velocity of the payload, which could be used to estimate the energy consumption. The required velocity for the payload to move on Γ_e at Q_1 can be obtained by using $R_2 = a(1-e^2)$ and Eqs. (2) and (6):

$$V'_{Q_1} = \left|\boldsymbol{V}'_{Q_1}\right| = \left[\mu\left(\frac{2}{R_1} - \frac{1}{a}\right)\right]^{0.5} = \left[\frac{\mu}{R_1}\left(\frac{1 + 2K + e^2}{1 + K}\right)\right]^{0.5} \tag{8}$$

Comparing with the velocity at Q_1 on Γ_i, i.e., $V_{Q_1} = (\mu/R_1)^{0.5}$, the required velocity change ΔV_{Q_1} for the payload can be easily derived from the cosine formula:

$$\Delta V_{Q_1} = \left[V_{Q_1}^2 + V_{Q_1}'^2 - 2V_{Q_1}V'_{Q_1}\cos\phi_1\right]^{0.5} = \left[V_{Q_1}^2 + V_{Q_1}'^2 - 2V_{Q_1}\left(\frac{H}{R_1}\right)\right]^{0.5} = \left[V_{Q_1}^2 + V_{Q_1}'^2 - 2V_{Q_1}\frac{[a\mu(1 - e^2)]^{0.5}}{R_1}\right]^{0.5} = \left[\left(\frac{\mu}{R_1}\right)\left(\frac{2 + 3K + e^2}{1 + K} - 2\sqrt{1 + K}\right)\right]^{0.5} \tag{9}$$

where ϕ_1 denotes the angle between $\boldsymbol{V}_{Q_1}$ and $\boldsymbol{V}'_{Q_1}$, that satisfying

$$\cos\phi_1 = \frac{1 + K}{\sqrt{1 + 2K + e^2}} \tag{10}$$

Following the same procedure, the velocity change ΔV_{P_2} of the payload at P_2 can be derived as follows:

$$V_{P_2} = \sqrt{\frac{\mu}{R_1}}\left(\frac{1 + e^2}{1 + K}\right)^{0.5} \tag{11}$$

$$V'_{P_2} = \sqrt{\frac{\mu}{R_1}}\frac{1}{(1 + K)^{0.5}} \tag{12}$$

$$\Delta V_{P_2} = \sqrt{\frac{\mu}{R_1}}\frac{e}{(1 + K)^{0.5}} \tag{13}$$

It is desired that the velocity change vector $\Delta\boldsymbol{V}_{P_2}$ can be realized by pulling the tether along the radial direction. On the other hand, $\Delta\boldsymbol{V}_{Q_1}$ may be accomplished by using some mechanism, such as a spring, on the spacecraft. The ejection angle of the payload relative to the velocity of the spacecraft at Q_1 (Fig. 3) can be computed as

$$\angle CBD = \phi_1 + \angle ACB$$

where $\angle ACB$ can be obtained from

$$\frac{\Delta V_{Q_1}}{\sin\phi_1} = \frac{V_{Q_1}}{\sin\angle ACB}$$

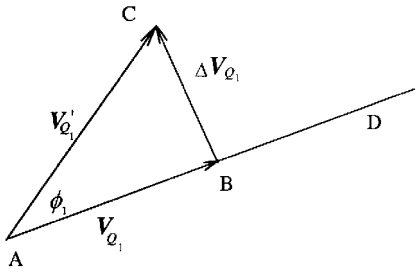

Fig. 3 Computation of ΔV_{Q_1}.

Thus,

$$\angle CBD = \arccos\left(\frac{1+K}{\sqrt{1+2K+e^2}}\right) + \arcsin\left[\frac{\sqrt{(e^2-K^2)/(1+2K+e^2)}}{\sqrt{(2+3K+e^2)/(1+K)-2\sqrt{1+K}}}\right] \tag{14}$$

To gain some physical insight into this strategy, the following example gives a set of designing parameters with R_1 and R_2 being 6800 and 6900 km, respectively. With $K = (R_2 - R_1)/R_1 = \frac{1}{68}$ and from the preceding equations, we obtain $e \simeq 0.0157517$, $\nu_1 \simeq -20.9957051$ deg, travel time $\simeq 1720.59$ s, $a \simeq 6901.712421$ km, $\phi_2 \simeq 0.902430$ deg, ejecting velocity $\Delta V_{Q_1} \simeq 70.612905$ m/s, and ejecting angle $\angle CBD \simeq 37.407491$ deg.

2. Ejecting the Payload at Q_2

Next, we investigate the possibility of ejecting the payload at Q_2, which may further save the time of deployment. For this case, Eqs. (1–3) are also applicable, and thus the true anomaly of P_2 corresponding to Γ_e is $\nu_2 = (\pi/2) \pm n\pi$. It is only necessary to modify Eq. (7), which becomes

$$\left(\arccos e - e\sqrt{1-e^2}\right) - \left(\frac{1-e^2}{1+K}\right)^{1.5}\left(\frac{\pi}{2} - \arccos\frac{K}{e}\right) = \arccos\left[\frac{e+(K/e)}{1+K}\right] - \frac{\sqrt{1-e^2}\sqrt{e^2-K^2}}{1+K} \tag{15}$$

to fulfill the flight time requirement. Numerical computations show that the LHS of Eq. (15) is always greater than the right-hand side (RHS) for any possible (e, K), with $K < e < 1$. This indicates that the flight time for the payload from Q_2 to P_2 is longer than that of the spacecraft along Γ_i from Q_2 to J_2. As a result, the orbit Γ_i cannot be adopted as the orbit of the spacecraft. Other transfer orbits taking the spacecraft from Q_2 to J_2 need to be designed to satisfy the equal-time constraint.

Because the motion around the apogee is slower, an elliptic orbit (denoted by Γ_{se}) for the spacecraft is sought with apogee close to Q_2. Let φ denote the angle between Q_2 and the apogee axis (Fig. 4). The true anomalies of Q_2 and J_2 corresponding to Γ_{se} are

$$\nu_{s1} = \pi - \varphi, \qquad \nu_{s2} = \pi + \varphi$$

respectively. On the other hand, the true anomaly of Q_2 with respect to Γ_e is $-\nu_1$, due to the symmetry of Q_1 and Q_2 relative to the perigee axis of Γ_e. Thus, $2\varphi = \nu_2 + \nu_1 = (\pi/2) + \nu_1$. By techniques similar to those used in the previous analysis, we obtain

$$a_{se} = R_1\frac{1+e_{se}\cos\nu_{s1}}{1-e_{se}^2}$$

where a_{se} and e_{se} are the semimajor axis and the eccentricity of Γ_{se}, respectively. The eccentric anomaly of Q_2 with respect to Γ_{se} is

$$E_{s1} = \arccos\left(\frac{e_{se}+\cos\nu_{s1}}{1+e_{se}\cos\nu_{s1}}\right)$$

Thus, the time required from the perigee of Γ_{se} to Q_2 is

$$\sqrt{\left(a_{se}^3/\mu\right)}(E_{s1} - e_{se}\sin E_{s1})$$

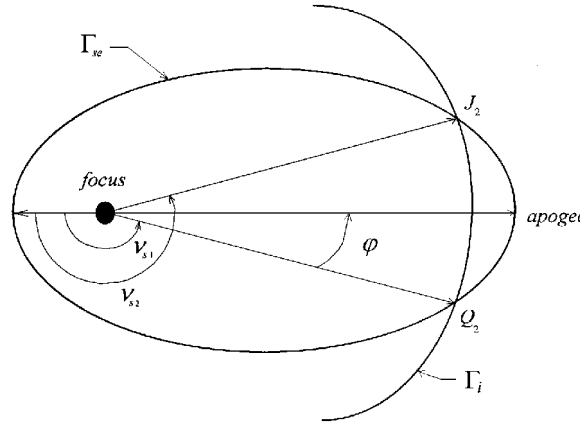

Fig. 4 Elliptic transfer orbit for the spacecraft.

By symmetry, $E_{s1} + E_{s2} = 2\pi$, where E_{s2} is the eccentric anomaly of J_2. The time elapsed for the spacecraft via Γ_{se} can then be derived as

$$2\sqrt{\left(a_{se}^3/\mu\right)}[\pi - (E_{s1} - e_{se}\sin E_{s1})] \tag{16}$$

Consequently, instead of Eq. (15), we have a modified equal-time constraint

$$2\sqrt{\frac{a_{se}^3}{\mu}}[\pi - (E_{s1} - e_{se}\sin E_{s1})] = \arccos e - e\sqrt{1-e^2} - \left\{\arccos\left[\frac{e+(K/e)}{1+K}\right] - \frac{\sqrt{1-e^2}\sqrt{e^2-K^2}}{1+K}\right\} \tag{17}$$

With given R_1 and R_2 and a suitably chosen e, Eq. (17) is solved for e_{se} varying between 0 and 1. Some numerical results are given subsequently. With $R_1 = 6800$ km, $R_2 = 6900$ km, the selection of $e = 0.06$ and $a = 6924.929747$ km yields $e_{se} = 0.0141644$ and $a_{se} = 6705.764746$ km; whereas the selection of $e = 0.1$ and $a = 6969.6969696$ km leads to $e_{se} = 0.0143752$ and $a_{se} = 6703.900033$ km.

Although the time of deployment for this strategy is shorter than the one discussed in Sec. III.A.1, the energy requirement is more demanding.

B. Hyperbolic Orbit

In addition to the elliptic orbits, hyperbolic orbits are also possibly chosen as transfer orbits. With similar deployment strategy, the orbit Γ_e is replaced by a hyperbolic orbit Γ_h in Fig. 2. Let $-a$, $-b$, and e be the semimajor axis, semiminor axis, and eccentricity of Γ_h, respectively, with $a, b < 0$. From the orbital equations, we have

$$r = \frac{H^2/\mu}{1+e\cos\nu} = \frac{p}{1+e\cos\nu} \qquad \text{with} \qquad p = H^2/\mu \tag{18}$$

where ν is the true anomaly, sometimes termed polar angle for hyperbola. With $x = r\cos\nu$ and $y = r\sin\nu$, Eq. (18) becomes

$$\frac{\{x - [ep/(e^2-1)]\}^2}{[p/(e^2-1)]^2} - \frac{y^2}{(p/\sqrt{e^2-1})^2} = 1 \tag{19}$$

Similar to the discussions on the elliptic orbits, the specifications described in the beginning of Sec. III are required to be satisfied. We also have

$$R_2 = \frac{p}{1+e\cos\nu_2} \tag{20}$$

$$H = \sqrt{\mu p} = R_2 V_{P_2}\cos\phi_2 \tag{21}$$

$$\sqrt{\mu/R_2} = V'_{P_2} = V_{P_2}\cos\phi_2 \tag{22}$$

where the variables are the same as defined in Sec. III.A. From Eqs. (20–22), we derive

$$R_2 = p, \qquad \nu_2 = (\pi/2) \pm n\pi$$

and choose $\pi/2$ for ν_2 in the following discussions. The branch of the hyperbola concave to the Earth can be expressed as

$$x - \frac{ep}{e^2-1} = -\frac{p}{e^2-1}\cosh F, \qquad y = \frac{p}{\sqrt{e^2-1}}\sinh F$$

which is parametrized by $F \in (-\infty, \infty)$, and

$$\cos\nu = \frac{e - \cosh F}{e\cosh F - 1}$$

Let the corresponding values of F for Q_1 and P_2 be F_1 and F_2, respectively. The time required for the payload moving from Q_1 to the perigee is then

$$\sqrt{(-a^3/\mu)}(-e\sinh F_1 + F_1)$$

Similarly, the time elapsed from the perigee to P_2 is

$$\sqrt{(-a^3/\mu)}(e\sinh F_2 - F_2)$$

As a result, the flight time requirement for the case of hyperbolic orbit leads to

$$\sqrt{(-a^3/\mu)}[e(\sinh F_2 - \sinh F_1) - (F_2 - F_1)] = \sqrt{\left(R_1^3/\mu\right)}(\nu_2 - \nu_1)$$

which is similar to Eq. (4). Noting $-a = p/(e^2-1)$, we obtain the equal-time constraint

$$\left(\frac{e^2-1}{1+K}\right)^{1.5}\left(\frac{\pi}{2} + \arccos\frac{K}{e}\right) = \left(e\sqrt{e^2-1} - \operatorname{arccosh} e\right) + \left\{\frac{\sqrt{e^2-K^2}}{1+K}\sqrt{e^2-1} - \operatorname{arccosh}\left[\frac{e+(K/e)}{1+K}\right]\right\} \tag{23}$$

where $K = (R_2 - R_1)/R_1$ as defined before.

Numerical computations (Fig. 5), in which the vertical axis denotes the value of the difference between the LHS and RHS of Eq. (23) and the abscissa is the eccentricity of Γ_h, show that there is no pair of (K, e) satisfying the constraint equation (23).

In fact, with $e > 1$, the travel time of the spacecraft is always longer than that of the payload's. Accordingly, to fulfill the equal-time constraint, suitable transfer orbits for the spacecraft need to be selected, which is analogous to Sec. III.A.2. It can be checked that elliptic orbits are not feasible, and thus hyperbolic orbits (denoted by Γ_{sh}) are adopted as the transfer orbits in this case. Let the semimajor axis and eccentricity of Γ_{sh} be $-a_{sh}$ and e_{sh}, respectively. Let ν_{s1}

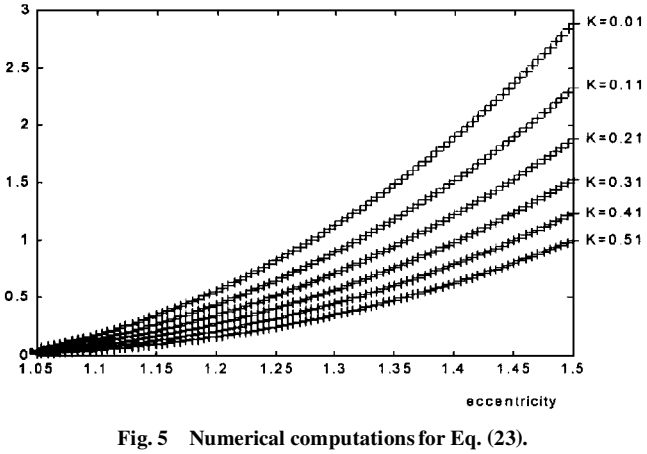

Fig. 5 Numerical computations for Eq. (23).

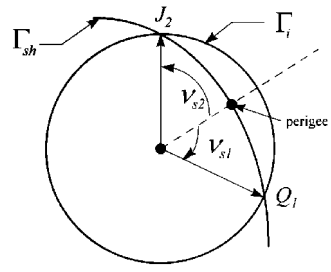

Fig. 6 Hyperbolic transfer orbit for the spacecraft.

and ν_{s2} denote the true anomaly of Q_1 and J_2 with respect to Γ_{sh}, respectively (Fig. 6). We have

$$-\nu_{s1} = \nu_{s2} = \frac{1}{2}\left(\frac{\pi}{2} - \nu_1\right), \qquad -a_{sh} = R_1\frac{1 + e_{sh}\cos\nu_{s2}}{e_{sh}^2 - 1}$$

$$\cos\nu_{s2} = \frac{e_{sh} - \cosh F_{s2}}{e_{sh}\cosh F_{s2} - 1}$$

where F_{s1} and F_{s2} are the parameters for Q_1 and J_2 with respect to Γ_{sh}, respectively. The time required for the spacecraft moving from Q_1 to J_2 along Γ_{sh} is

$$2\sqrt{\frac{-a_{sh}^3}{\mu}}(e_{sh}\sinh F_{s2} - F_{s2})$$

The equal-time constraint becomes

$$2\sqrt{\frac{-a_{sh}^3}{\mu}}(e_{sh}\sinh F_{s2} - F_{s2}) = \sqrt{\frac{-a^3}{\mu}}\left[\left(e\sqrt{e^2-1} - \operatorname{arccosh} e\right) + \left\{\frac{\sqrt{e^2-K^2}}{1+K}\sqrt{e^2-1} - \operatorname{arccosh}\left[\frac{e+(K/e)}{1+K}\right]\right\}\right] \tag{24}$$

Numerical computations were performed to check whether Eq. (24) is solvable. For $R_1 = 6800$ km and $R_2 = 6900$ km, we found that $e = 1.2$, $a = -15681.8181$ km, $\Rightarrow e_{sh} = 1.1796$, $a_{sh} = -17489.6792$ km and $e = 1.4$, $a = -7187.5$ km, $\Rightarrow e_{sh} = 1.3776$, $a_{sh} = -7627.3414$ km. As a consequence, such strategy for deployment is possible.

It has been checked that the time required for the spacecraft moving along Γ_i is greater than that for the payload moving along Γ_h. Thus, we examine the possibility of ejecting the payload at Q_2. Equation (23) needs to be updated as

$$\left(\frac{e^2-1}{1+K}\right)^{1.5}\left(\frac{\pi}{2} - \arccos\frac{K}{e}\right) = \left(e\sqrt{e^2-1} - \operatorname{arccosh} e\right) - \left\{\frac{e^2-K^2}{1+K}\sqrt{e^2-1} - \operatorname{arccosh}\left[\frac{e+(K/e)}{1+K}\right]\right\} \tag{25}$$

However, numerical calculations showed that the travel time of the spacecraft is always less than that of the payload's for any pair of (K, e). Accordingly, the strategy of ejecting the payload at Q_2 along Γ_h, with the spacecraft staying on Γ_i, is not feasible to meet all of the requirements.

Finally, we consider the case that Γ_h is tangent to Γ_i, which leads to $e = K$ at $Q_1 (= Q_2)$. By similar analysis and numerical computations, it is shown that the strategy of having the spacecraft moving on Γ_i is not feasible. Consequently, if only the payload is allowed to change its orbit, the hyperbolic orbits cannot be adopted.

Various possibilities to find suitable orbits to solve the deployment problem have been pursued. Recall that Lambert's problem is to obtain a transfer orbit that connects two points in space within a specified period.[22] Here, the deployment problem has two main distinct features. First, the flight time for completing the mission is not prescribed; it is, however, solved in the process. Second, the point of pulling the tether at the end of the mission needs to be carefully designed to fulfill the velocity change condition. This somewhat reveals the fact that the problem we are dealing with includes two interacting bodies, instead of an individual one.

IV. TSS Deployment

In Secs. III.A and III.B, it is required that at the end of the deployment phase, the payload at P_2 must have the desired velocity $V'_{P_2} = \sqrt{(\mu/R_2)}$, i.e., Eqs. (3) and (22). However, in NASA's TSS plan, the station-keeping mode demands that the TSS system should not only keep the Earth-pointing attitude but also move around the Earth with a common angular velocity $\omega_{\rm TSS}$. Thus, the desired velocity of the payload in the third requirement of the deployment problem stated earlier should be $\omega_{\rm TSS} R_2$. Taking the tension force distributed along the tether into consideration, $\omega_{\rm TSS}$ can be calculated from[23]

$$\mu = \omega_{\rm TSS}^2 |\boldsymbol{r}_g| (\boldsymbol{r}_g \cdot \boldsymbol{r}_c) \tag{26}$$

where $\boldsymbol{r}_g$ and $\boldsymbol{r}_c$ are the position vectors of the center of gravity and the center of mass of TSS with respect to an inertial coordinate system with its origin at the Earth center, respectively. The preceding formula can be simplified as $\omega_{\rm TSS}^2 = \mu/|\boldsymbol{r}_c|^3$, i.e., Kepler's third law, if the system consists of one particle only, in which $\boldsymbol{r}_g = \boldsymbol{r}_c$. Thus, if Eq. (26) is adopted, V'_{P_2} should be changed to $\omega_{\rm TSS} R_2$, which is different from $\sqrt{(\mu/R_2)}$. Accordingly, an example is explored here to examine whether the proposed deployment strategy is feasible. First, some realistic parameters for TSS are selected as follows: $m_1 = 80{,}000$ kg, $m_2 = 500$ kg, $m_t = 8.2$ kg/km, $R_1 = 6800$ km, $R_2 = 6900$ km, and $d_t = 2.54$ mm, where m_t and d_t denote the mass density and the diameter of the tether, respectively. Second, in view of the Earth-pointing attitude for TSS in station-keeping mode, all of the position vectors of the elements in TSS are along a radial direction. We can then obtain $|\boldsymbol{r}_c| = 6801.119$ km and $|\boldsymbol{r}_g| = 6801.0986$ km, respectively. From Eq. (26), we have $\omega_{\rm TSS} = 1.1256 \times 10^{-3}$ rad/s, and thus $V'_{P_2} = 7.7669$ km/s. Note that 7.7669 km/s is larger than $\sqrt{(\mu/R_2)} = 7.6005$ km/s, which is the velocity of Γ_o. For the latter case, Table 1 in Sec. III.A shows that a feasible elliptic transfer orbit exists, with the payload being ejected at Q_1 and the spacecraft staying on Γ_i. However, due to the faster speed at the current situation, it is suspected that we may need to eject the payload at Q_2 or change the orbit of the spacecraft to meet the equal-time constraint.

Following the methodologies stated in Sec. III.A, we consider first the case in which the payload is ejected at Q_2 along a transfer orbit Γ_e while the spacecraft moves on Γ_i. Equation (3) is now replaced by

$$\omega_{\rm TSS} R_2 = \sqrt{\mu[(2/R_2) - (1/a)]} \cos\phi_2 = 7.7669\,\text{km/s}$$

From Eqs. (1) and (2), we have the orbit equation for Γ_e:

$$R = \frac{7205.35}{1 + e\cos\nu}$$

Let ν_1 and ν_2 denote the true anomalies of Q_2 and P_2 corresponding to Γ_e, respectively. We have

$$R_1 = \frac{7205.35}{1 + e\cos\nu_1}, \qquad R_2 = \frac{7205.35}{1 + e\cos\nu_2}$$

Evidently, neither $\cos\nu_1$ nor $\cos\nu_2$ can be zero, which indicates that $\nu_2 \neq (\pi/2) \pm n\pi$. It can be further shown that the equal-time constraint for the current situation becomes

$$\sqrt{\frac{R_1^3}{\mu}}(\nu_2 - \nu_1) = \sqrt{\frac{(7205.35)^3}{\mu(1-e^2)^3}}[(E_2 - e\sin E_2) - (E_1 - e\sin E_1)] \tag{27}$$

with

$$\cos E_i = \frac{e + \cos\nu_i}{1 + e\cos\nu_i}, \qquad i = 1, 2$$

Numerical computations show that this condition cannot be satisfied for any

$$K < \frac{7205.35 - R_1}{R_1} \leq e \leq 1$$

As a result, an elliptic transfer orbit Γ_{se} needs to be designed for the spacecraft to complete the deployment process and meet the specifications. It is desired that the perigee of Γ_{se} is chosen to be close to Q_2, which leads to the reduction of the traveling time of the spacecraft. Analogous to the discussions in Sec. III.A, the condition to fulfill the requirements can be found to be

$$2\sqrt{\frac{a_{se}^3}{\mu}}(E_{s2} - e_{se}\sin E_{s2}) = \sqrt{\frac{(7205.35)^3}{\mu(1-e^2)^3}}[(E_2 - e\sin E_2) - (E_1 - e\sin E_1)]$$

with

$$\cos E_{s2} = \frac{e_{se} + \cos[(\nu_2 - \nu_1)/2]}{1 + e_{se}\cos[(\nu_2 - \nu_1)/2]}$$

and

$$a_{se} = \frac{1 + e_{se}\cos[(\nu_2 - \nu_1)/2]}{1 - e_{se}^2} R_1$$

Numerical computations give rise to the following pair of the possible transfer orbits Γ_e and Γ_{se}. For Γ_e, transfer orbit for the payload: $e = 0.07$, $a = 7240.8292$ km, $\nu_1 = 31.6167$ deg, $\nu_2 = 50.7879$ deg, $\Delta V_{Q_2} = 353.6447$ m/s, $\Delta V_{P_2} = 403.366$ m/s, and time elapsed $= 292.6731$ s. For Γ_{se}, transfer orbit for the spacecraft: $e_{se} = 0.03033$, $a_{se} = 7009.82629$ km, $\nu_{s1} = -9.58558$ deg, $\nu_{s2} = 9.58558$ deg, $\Delta V_{sQ_2} = 119.838$ m/s, $\Delta V_{J_2} = 121.67$ m/s, and time elapsed $= 292.6731$ s. In our strategy, ΔV_{P_2} is to be realized by pulling the tether when TSS arrives at Earth-pointing attitude, which may lead to some concerns on the breakage of the tether. The tensile stress σ of the tether at the moment of pulling is next estimated. Letting Δt be the time duration for the pulling process, the tension force F is obtained from

$$F \cdot \Delta t = m_2 \cdot \Delta V_{P_2}$$

With assumed $d_t = 2.54$ mm, the associated tensile stress is $\sigma = (1/\Delta t)38.9$ GPa. The tether must be strong enough to resist the tensile stress in the time duration Δt. If this is not the case in practical situations, we may split the deployment strategy into a series of successive steps. A collection of transfer orbits may be found such that the tensile stress can be controlled under the yield strength of the tether at each pulling. This delicate process, however, needs further investigations.

V. Retrieval Phase

The preceding section shows that the passive maneuvering strategies proposed in Sec. III are effective for the TSS deployment problem. The possibility of similar ideas in solving the retrieval problem for TSS is explored in this section.

Let the TSS model in Sec. IV be considered again. Before the retrieval phase, the TSS is assumed to move around the Earth with the Earth-pointing attitude. As the payload arrives at P_1 and the spacecraft arrives at J_1 (Fig. 2), the first step is to pull the tether such that the payload's velocity $\omega_{\rm TSS} R_2$ on Γ_o can be changed to the velocity $\sqrt{\mu[(2/R_2) - (1/a)]}$ on Γ_e. With the values $\omega_{\rm TSS}$, R_2, . . ., etc., calculated in Sec. IV and Eqs. (1) and (2), the orbit equation for Γ_e becomes

$$R = \frac{7205.35}{1 + e\cos\nu}$$

Letting $\nu_1 \leq 0$ and $\nu_2 \leq 0$ be the true anomalies of P_1 and Q_1 corresponding to Γ_e, respectively, we have

$$R_2 = \frac{7205.35}{1 + e\cos\nu_1}, \qquad R_1 = \frac{7205.35}{1 + e\cos\nu_2}$$

If it is desired that the payload can intercept the spacecraft at Q_1, the last requirement is to have the flight time of the spacecraft from

J_1 to Q_1 be equal to that of the payload from P_1 to Q_1. Thus, the equal-time constraint becomes

$$\sqrt{\frac{R_1^3}{\mu}}(\nu_2 - \nu_1)$$
$$= \sqrt{\frac{(7205.35)^3}{\mu(1-e^2)^3}}[(-E_2 + e\sin E_2) - (-E_1 + e\sin E_1)]$$
$$= \sqrt{\frac{(7205.35)^3}{\mu(1-e^2)^3}}[(E_1 - e\sin E_1) - (E_2 - e\sin E_2)] \qquad (28)$$

with

$$\cos(-E_i) = \frac{e + \cos\nu_i}{1 + e\cos\nu_i}, \qquad i = 1, 2$$

where $-E_1$ and $-E_2$ are the eccentric anomalies of P_1 and Q_1, respectively. By the symmetry of Γ_e, it is readily observed that E_1 and E_2 are the eccentric anomalies of P_2 and Q_2, respectively. Thus, Eq. (28) is nothing but the equation to be solved for the deployment problem that the payload leaves the spacecraft at Q_2 and arrives at P_2 while the spacecraft moves to J_2. Therefore, the retrieval procedure is simply the reverse of the deployment procedure. The transfer orbits found in Sec. IV can also be used for the retrieval phase.

In the literature, it is observed that the shortening of the tether may cause instability during the retrieval phase. This is due to the coupling between the tether, the payload, and the spacecraft. However, in the strategy proposed in this paper, the tether keeps slack during the transfer orbit, which alleviates the interactions. The instability problem can then possibly be avoided.

VI. Conclusions

New strategies for the maneuvering of a tether-connected system were proposed. The analysis and numerical results showed that such strategies are possible. The tether deployed in the TSS-1 mission attained only 256 m. Although the investigation report said that the failure was mainly due to a mechanical problem, the dynamical behavior was observed to be quite complicated. A recent attempt of TSS deployment also failed, and further studies are necessary. The passive scheme presented is simple and reliable and may be adopted in the future mission of TSS.

Acknowledgment

This work was partially supported by the National Science Council, Taiwan, Republic of China, under Grant NSC84-2121-M-002-013.

References

[1]Colombo, G., et al., "Shuttle-Borne 'Skyhook': A New Tool for Low-Orbital-Altitude Research," Smithsonian Inst. Astrophysical Observatory, SAO Rept., Sept. 1974.

[2]Misra, A. K., and Modi, V. J., "Deployment and Retrieval of Shuttle Supported Tethered Satellites," *Journal of Guidance, Control, and Dynamics*, Vol. 5, No. 3, 1982, pp. 278–285.

[3]Misra, A. K., and Modi, V. J., "A Survey on the Dynamics and Control of Tethered Satellite," *Tethers in Space*, American Astronautical Society, San Diego, CA, 1986, pp. 667–719.

[4]Arnold, D. A., "The Behavior of Long Tethers in Space," *Journal of the Astronautical Sciences*, Vol. 35, No. 1, 1987, pp. 3–18.

[5]Bainum, P. M., and Kumar, V. K., "Optimal Control of the Shuttle-Tethered-Subsatellite," *Acta Astronautica*, Vol. 7, No. 12, 1980, pp. 1333–1348.

[6]Banerjee, A. K., and Kane, T. R., "Tether Deployment Dynamics," *Journal of the Astronautical Sciences*, Vol. 30, No. 4, 1982, pp. 347–365.

[7]Chernous'ko, F. L., "Dynamics of Retrieval of a Space Tethered System," *Prikladnaya Matematika y Mekanika* [*Applied Mathematics and Mechanics*], Vol. 59, No. 2, 1995, pp. 165–173.

[8]Andreas, H., and Williamson, P. R., "Deployment of a Tethered Satellite Pair Into Low Earth Orbit for Plasma Diagnostics," *Journal of the Astronautical Sciences*, Vol. 34, No. 1, 1986, pp. 65–90.

[9]Kane, T. R., and Levinson, D. A., "Deployment of a Cable-Supported Payload from an Orbiting Spacecraft," *Journal of Spacecraft and Rockets*, Vol. 14, No. 7, 1977, pp. 409–413.

[10]Levin, E. M., "Nearly-Uniform Deployment Strategy for Space Tether System," *Acta Astronautica*, Vol. 32, No. 5, 1994, pp. 399–403.

[11]Netzer, E., and Kane, T. R., "Deployment and Retrieval Optimization of a Tethered Satellite System," *Journal of Guidance, Control, and Dynamics*, Vol. 16, No. 6, 1993, pp. 1085–1091.

[12]Peláez, J., "On the Dynamics of the Deployment of a Tether from an Orbiter—I. Basic Equations," *Acta Astronautica*, Vol. 36, No. 2, 1995, pp. 113–122.

[13]Penzo, P. A., and Ammann, P. W. (eds.), *Tethers In Space Handbook*, 2nd ed., NASA Office of Space Flight Advanced Program Development, 1989, pp. 150–160.

[14]Rupp, C. C., and Laue, J. H., "Shuttle/Tethered Satellite System," *Journal of the Astronautical Sciences*, Vol. 26, No. 1, 1978, pp. 1–17.

[15]Fujii, H. A., and Anazawa, S., "Deployment/Retrieval Control of Tethered Subsatellite Through an Optimal Path," *Journal of Guidance, Control, and Dynamics*, Vol. 17, No. 6, 1994, pp. 1292–1298.

[16]Netzer, E., and Kane, T. R., "Estimation and Control of Tethered Satellite Systems," *Journal of Guidance, Control, and Dynamics*, Vol. 18, No. 4, 1995, pp. 851–858.

[17]Banerjee, A. K., and Kane, T. R., "Tethered Satellite Retrieval with Thruster Augmented Control," *Journal of Guidance, Control, and Dynamics*, Vol. 7, No. 1, 1984, pp. 45–50.

[18]Pines, D. J., von Flotow, A. H., and Redding, D. C., "Two Nonlinear Control Approaches for Retrieval of a Thrusting Tethered Subsatellite," *Journal of Guidance, Control, and Dynamics*, Vol. 13, No. 4, 1990, pp. 651–658.

[19]Vadali, S. R., and Kim, E.-S., "Feedback Control of Tethered Satellite Using Lyapunov Stability Theory," *Journal of Guidance, Control, and Dynamics*, Vol. 14, No. 4, 1991, pp. 729–735.

[20]Wang, L. S, Chern, S. J., and Shih, C. W., "On the Dynamics of a Tethered Satellite System," *Archive for Rational Mechanics and Analysis*, Vol. 127, 1994, pp. 297–318.

[21]Wiesel, W. E., *Spaceflight Dynamics*, McGraw–Hill, New York, 1992, pp. 54–57.

[22]Battin, R. H., "Lambert's Problem Revisited," *AIAA Journal*, Vol. 15, No. 5, 1977, pp. 707–713.

[23]Wang, L. S., and Cheng, S. F., "Dynamics of Spring-Connected Masses in Orbit," *Celestial Mechanics and Dynamical Astronomy*, Vol. 63, 1996, pp. 289–312.